Nanostructured gradient-index antireflection diffractive optics

Chih-Hao Chang,[1,*] Jose A. Dominguez-Caballero,[1] Hyungryul J. Choi,[1] and George Barbastathis[1,2]

[1]Department of Mechanical Engineering, Massachusetts Institute of Technology, Cambridge, Massachusetts 02139, USA

[2]Singapore-MIT Alliance for Research and Technology (SMART) Centre, Singapore

*Corresponding author: chichang@mit.edu

Received March 18, 2011; accepted May 8, 2011;
posted May 19, 2011 (Doc. ID 144432); published June 15, 2011

We describe the fabrication and characterization of a nanostructured diffractive element with near-zero reflection losses. In this element, subwavelength nanostructures emulating adiabatic index matching are integrated on the surface of a diffractive microstructure to suppress reflected diffraction orders. The fabricated silicon grating exhibits reflected efficiencies that are suppressed by 2 orders of magnitude over broad wavelength bands and wide incident angles. Theoretical models of the fabricated structure based on rigorous coupled-wave analysis and effective medium theory are in agreement with the experimental data. The proposed principles can be applied to improve the performance of any diffractive structures, potentially leading to more efficient Fresnel lenses, holographic elements, and integrated optical systems. © 2011 Optical Society of America

OCIS codes: 050.1950, 310.6628, 310.1210.

In recent years there has been significant interest in broadband, omnidirectional antireflection (AR) nanostructures that minimize Fresnel reflection due to index mismatch [1–8]. The reflection can be suppressed by using adiabatic impedance matching implemented as an intermediate material with gradually varying index in the direction of surface normal. Subwavelength structure is an effective method to implement such a gradient-index (GRIN) surface, and various techniques such as nanolithography [1,2], multilayer porous films [3,4], self-masking plasma etching [5], polymer replication [6], and colloidal assembly [7,8] have been demonstrated.

However, these recent studies have been restricted to planar surfaces. Diffractive optical elements such as diffraction gratings, Fresnel zone plates, and holographic optics also suffer from Fresnel reflection losses evidenced as undesirable reflection orders. Recently, we proposed a new class of GRIN diffractive optics that is capable of suppressing such reflection losses [9]. Using the same GRIN principles, we numerically demonstrated diffractive elements where 100% of the incident energy is transmitted. Here we present the fabrication and testing of such a nanostructured GRIN grating with suppressed reflected orders. There are many potential applications, such as higher efficiency solar cells based on diffractive optics [10,11] and grating couplers for integrated optical systems [12].

The proposed nanostructured GRIN grating is illustrated in Fig. 1(a). To implement the GRIN, subwavelength tapered nanostructures are integrated on both the ridge and groove of the grating. The fabrication process of the nanostructured grating is illustrated in Figs. 1(b)–1(e). First, monodispersed polystyrene nanospheres [13] with subwavelength diameter are spincoated on a silicon substrate with 240 nm hydrogen silsesquioxane (HSQ), as shown in Fig. 1(b). The pattern is transferred into HSQ and silicon using CHF_3 and HBr reactive ion etching (RIE), respectively. The high etch selectivity between silicon and HSQ during the HBr RIE results in high aspect-ratio tapered nanostructures, as shown in Fig. 1(c). The substrate is then planarized by an antireflection coating (ARC) layer, and the grating structure patterned using contact lithography, shown in Fig. 1(d). The planarization polymer is removed and the grating structure etched into the silicon substrate with O_2 and HBr RIE, respectively, as shown in Fig. 1(e).

Micrographs of the fabricated silicon GRIN grating is depicted in Fig. 2. The grating has a period of 5 μm and the subwavelength cone-shaped pillars have nominal base diameter of 150 nm. The micrograph in Fig. 2(a) illustrates that the fabricated structure resembles a grating with nanoengineered surfaces. A cross-sectional micrograph is shown in Fig. 2(b), where the cone heights on the ridge and groove are 650 and 600 nm, respectively. The structure inside the groove has a slightly different profile and is shorter due to longer etch time. A higher magnification micrograph of the nanostructure on the ridge and groove are shown in Figs. 2(c) and 2(d), respectively. Some point defects can be observed, characteristic of nanosphere self-assembly. As a result the nanostructure is not perfectly periodic and some scattering is expected, reducing the total power going into the transmitted orders.

The reflected efficiencies of the fabricated structure are measured as functions of incident angle, as shown in Fig. 3. The incident light has $\lambda = 633$, 532, and 351 nm from HeNe, frequency-doubled Nd:YAG, and Argon ion lasers, respectively, with both TE and TM polarizations plotted separately. The solid circles represent the measured zeroth and $\pm$1st orders, and the open circles illustrate the efficiency data measured for a bare silicon grating. The solid and dashed lines are the corresponding theoretical simulations for the gratings using rigorous coupled-wave analysis (RCWA) [14]. In this model, the subwavelength nanostructures are approximated by five discrete homogeneous layers and their indices are approximated using effective medium theory [15]. An optimization routine was used to fit the thickness and duty-cycle of each layer to the measured data. The resulting cone stack parameters are listed in Table 1. Two different

0146-9592/11/122354-03$15.00/0 © 2011 Optical Society of America

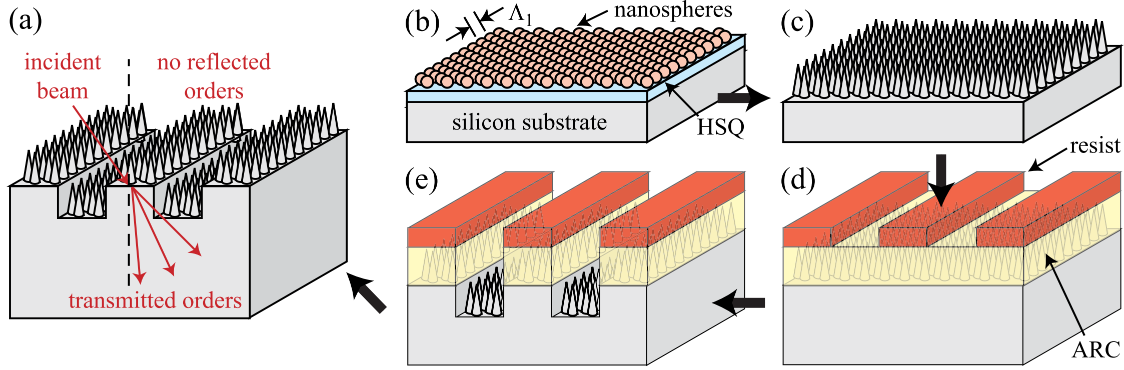

Fig. 1. (Color online) (a) Schematic of the proposed nanostructured GRIN grating, where the reflected orders are suppressed and all energy is transmitted. (b)–(e) Fabrication process of the grating in silicon. (b) Nanospheres are spincoated on a HSQ-coated silicon substrate, and (c) the subwavelength features are etched into the substrate. (d) The substrate is then planarized, and the diffractive microstructure patterned using contact lithography and (e) transferred using RIE.

cone stack geometries were used to match the difference in profiles of the fabricated structures on the ridge and groove, as mentioned earlier. The measurements indicated suppression by at least 2 orders of magnitude in the reflected orders of the GRIN grating over a large range of incident angles up to 60°.

Pictures of the fabricated sample next to a Si grating are shown in Fig. 4. In Fig. 4(a), a broadband fiber light source illuminates the samples at near normal incidence at the sample interface, while in Fig. 4(b) the samples were illuminated by normal room lighting. In both cases the AR GRIN grating appears dark because the reflected diffraction orders have been suppressed. In Figure 4(a), the specular reflected zeroth and color-dispersed first diffracted order can be clearly observed on the bare Si grating, but are barely visible on the AR GRIN grating. Note that in this wavelength range silicon absorbs all transmitted orders and thus it is not suitable for transmissive elements, but it can be used in

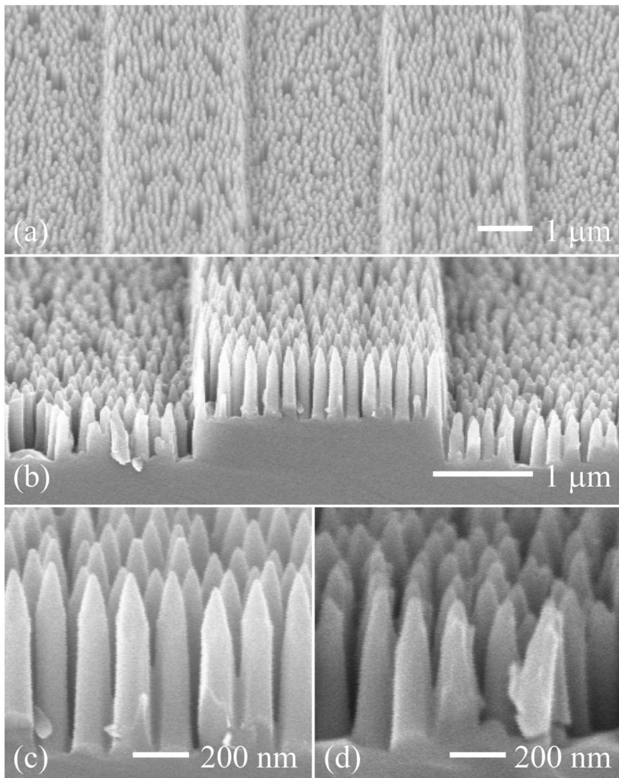

Fig. 2. (Color online) Micrographs of fabricated nanostructured GRIN grating. (a) Top view of the 5 μm-period grating with nanoengineered surfaces. (b) Cross-section view of the structure, the grating depth is around 570 nm. The cones on the grating (c) ridge and (d) groove have base diameter of 150 nm and heights of 650 and 570 nm, respectively.

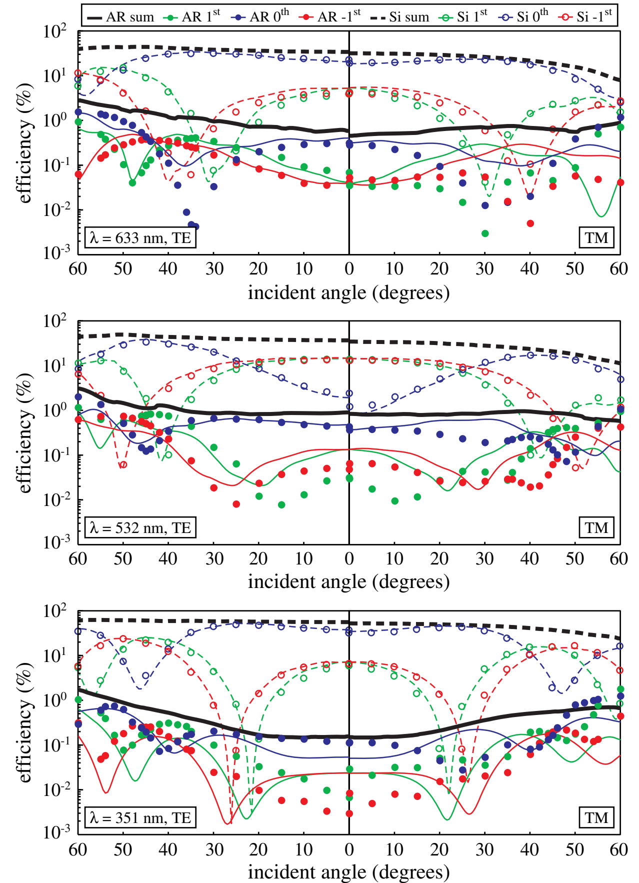

Fig. 3. (Color online) Measured reflected efficiencies of the zeroth and ±1st diffracted orders for the AR and silicon grating for incident wavelengths of 633, 532, and 351 nm. The solid and dashed lines are simulated efficiencies using RCWA and EMT.

Table 1. Parameters of the Numerical Model

	Ridge		Groove	
Layers	d_r (nm)	f_r	d_g (nm)	f_g
1	123	0.18	99	0.27
2	117	0.47	87	0.52
3	65	0.73	51	0.80
4	45	0.90	40	0.91
5	308	0.97	295	0.98

absorptive applications such as absorption enhancing diffractive structures [10,11]. Nonabsorbing substrate material can be used to construct a transmissive diffractive element.

In this work the fabricated structure is not perfectly periodic; the average spacing is approximately 150 nm. It is important to note that while the structure is subwavelength in air for the wavelength range tested, it becomes diffractive in the higher–index silicon material. This effect is expected to result in additional scattering in the transmitted orders. To ensure proper subwavelength operation, the dimensions of the structure should be further reduced to sub-100 nm length scale. This is outside the scope of this work, and is currently under investigation.

We have demonstrated the suppression of reflected diffraction orders from a diffraction grating by using nanostructured materials. In the fabricated element, subwavelength tapered nanostructure were integrated on the grating surface to provide adiabatic impedance matching in the form of a GRIN medium. The fabricated nanostructured grating demonstrates suppression of all reflected orders by 2 orders of magnitude for broad wavelength bands and large incident angles. The concept demonstrated herein for periodic binary gratings can be applied to other types of diffractive optics, for example Fresnel zone plates, blazed gratings, and computer–generated holograms.

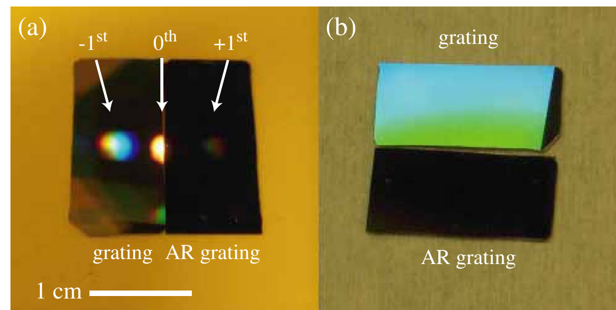

Fig. 4. (Color online) Images of the fabricated AR grating next to a bare silicon grating under (a) white fiber source at normal incidence. Both zeroth and first orders are suppressed in the AR grating sample. (b) The fabricated structure also demonstrates suppressed diffraction in normal room lighting.

References

1. P. Lalanne and G. M. Morris, Nanotechnology **8**, 53 (1997).
2. Y. Kanamori, M. Sasaki, and K. Hane, Opt. Lett. **24**, 1422 (1999).
3. J.-Q. Xi, M. F. Schubert, J. K. Kim, E. F. Schubert, M. Chen, S.-Y. Lin, W. Liu, and J. A. Smart, Nat. Photon. **1**, 176 (2007).
4. M.-L. Kuo, D. J. Poxson, Y. S. Kim, F. W. Mont, J. K. Kim, E. F. Schubert, and S.-Y. Lin, Opt. Lett. **33**, 2527 (2008).
5. Y.-F. Huang, S. Chattopadhyay, Y.-J. Jen, C.-Y. Peng, T.-A. Liu, Y.-K. Hsu, C.-L. Pan, H.-C. Lo, C.-H. Hsu, Y.-H. Chang, C.-S. Lee, K.-H. Chen, and L.-C. Chen, Nature Nanotechnology **2**, 770 (2007).
6. G. Xie, G. Zhang, F. Lin, J. Zhang, Z. Liu, and S. Mu, Nanotechnology **19**, 095605 (2008).
7. Y. Zhao, J. Wang, and G. Mao, Opt. Lett. **30**, 1885 (2005).
8. H. L. Chen, S. Y. Chuang, C. H. Lin, and Y. H. Lin, Opt. Express **15**, 14793 (2007).
9. C.-H. Chang, L. Waller, and G. Barbastathis, Opt. Lett. **35**, 907 (2010).
10. H. Stiebig, N. Senoussaoui, C. Zahren, C. Haase, and J. Müller, Prog. Photovoltaics **14**, 13 (2006).
11. C. Eisele, C. E. Nebel, and M. Stutzmann, J. Appl. Phys. **89**, 7722 (2001).
12. D. Taillaert, P. Bienstman, and R. Baets, Opt. Lett **29**, 2749 (2004).
13. J. C. Hulteen and R. P. Van Duyne, J. Vac. Sci. Technol. A **13**, 1553 (1995).
14. M. G. Moharam, E. B. Grann, D. A. Pommet, and T. K. Gaylord, J. Opt. Soc. Am. A **12**, 1068 (1995).
15. F. T. Chen and H. G. Craighead, Opt. Lett. **20**, 121 (1995).